KSME

Springer

Journal of Mechanical Science and Technology 34 (4) 2020

Original Article
DOI 10.1007/s12206-020-0317-y

Keywords:
· Structural reliability
· Kriging metamodel
· Active learning
· Monte Carlo
· Failure probability

Correspondence to:
Hong Linxiong
honglinxiong@mail.nwpu.edu.cn

Citation:
Linxiong, H., Huacong, L., Kai, P., Hongliang, X. (2020). A novel kriging based active learning method for structural reliability analysis. Journal of Mechanical Science and Technology 34 (4) (2020) 1545~1556.
http://doi.org/10.1007/s12206-020-0317-y

Received November 18th, 2019
Revised January 25th, 2020
Accepted February 4th, 2020

† Recommended by Editor Chongdu Cho

A novel kriging based active learning method for structural reliability analysis

Hong Linxiong, Li Huacong, Peng Kai and Xiao Hongliang

School of Power and Energy, Northwestern Polytechnical University, Xi'an 710072, China

Abstract In the reliability analysis of engineering structures, there are usually implict and highly nonlinear performance function problems, which leads to the time-consuming computations. In this paper, a novel Kriging based reliability analysis method combined with the improved efficient global optimization (IEGO) and a secondary point selection strategy is proposed. Based on the IEGO algorithm, the expected improvement function is redefining, which will focus on the points both with large variance and near the limit state surface. Moreover, a secondary point selection strategy is raised to find the point with larger expected improvement and closed to the limit state surface, which can further improve the efficiency of the active learning process. Five examples indicates that the raised method has satisfactory global and local search capability, and can evaluate the probability of failure efficiently.

1. Introduction

Through the advancement of structural engineering technology, the structural complexity also increases, resulting in highly nonlinear and implicit performance functions of the product. In general, some real response values can only be obtained by finite element analysis or test which leads to larger computation. Therefore, a variety of analytical techniques have been developed to evaluate the reliability of complex structures.

The earliest, a numerical simulation method named Monte Carlo simulation (MCS) was introduced into the reliability analysis that can estimate the failure probability precisely [1]. However, the MCS is used on the premise of a large number of calls to the performance function which may lead to time-consuming problem. As a result, many other improved sampling methods have appeared, e.g. subset simulation (SS) [2, 3], importance sampling (IS) [3, 4] and line sampling (LS) [5, 6]. While all these improving methods cannot satisfy the requirements of calculation efficiency in some more complexity reliability problems. Then, some analytic methods like the first-order reliability method (FORM) is proposed, which is an approximate solution based on the Taylor expansion theory [7], can greatly reduce the calling times of performance function. Yet this method may result in low calculation accuracy when dealing with complex nonlinear structures, and it can't be applied to implicit problems.

For solving the problems of computational cost and implicit performance function, it is more and more important to develop the surrogate method, which is to use an artificial approximation model to fit and approximate the implicit relationship between input and output of real structure. The surrogate model with sufficient simulation accuracy for the real structure can be used to replace the performance function of real structure, which not only reduces the real performance function callings but also can accurately estimate the failure probability. In recent years, various surrogate models have been proposed to replace the real performance function, such as response surface method (RSM) [8-10], support vector machine (SVM) [11-13], artificial neural network (ANN) [14-16] and Kriging metamodel [4, 17-19]. And the Kriging metamodel is adopted in this research.

Kriging, first proposed by Krige [20], is a spatial interpolation technique, which can give optimal linear unbiased estimates in particular stochastic processes. Furthermore, the Kriging model can provide both the predicted response in unknown points and the local variance of the

predicted response value. Due to the excellent characteristics, the Kriging model has been applied in reliability analysis for a long time. To improve the solving performance of the Kriging in reliability engineering, multiple methods of constructing the Kriging model have been developed, which can be roughly separated into 3 categories:

(1) Optimizing the parameters of correlation function with the intelligent optimization algorithm. Liu et al. introduced an artificial bee colony algorithm to improve the efficiency of parameter solving, and effectively ensure the optimal unbiasedness of Kriging model prediction results [21]. Wei et al. use the particle swarm optimization-simulated annealing (PSOSA) algorithm for the optimization of the correlation parameters [22]. And the results pointed out that the optimization algorithm can improve the calculation efficiency greatly.

(2) To optimize the parameters of the metamodel itself, a sequentially learning mechanism based on the Kriging model was developed. Efficient global optimization, construct an expected improvement (EI) function for sequential learning, which is developed by Jones et al. [23]. However, the EGO is not suitable for reliability analysis, due to the sampling area of this learning function doesn't fully meet the requirements of reliability analysis. Inspired by the EGO method, Bichon et al. introduced the efficient global reliability analysis (EGRA) into structural reliability analysis [24], with an efficient expected feasibility function (EFF). The EFF searches for points among candidates that are with larger variance and near the limit state surface (LSS). Another active learning function U [19], raised by Echard et al., concentrates on the point with a high probability of misclassification on the sign of response value. Lv et al. also present a novel active learning method H based on the information entropy [25], which can measure the predicted uncertainty among the candidate points and help construct the Kriging model precisely near the LSS.

(3) The last major research area is the sampling method. As we know, the sampling method is applied in both the construction of the candidate point set and the calculation of failure probability. In general, the Latin hypercube sampling (LHS) and MCS can be applied in developing the initial point set, called the initial design point. And, different sampling methods like MCS, IS, SS, LS and subset simulation importance sampling (SSIS) are combined with the Kriging model respectively to calculate the structural reliability index [25-29].

In this paper, an improved active learning function EH and a secondary point selection strategy are developed to update the Kriging metamodel iteratively. Firstly, assuming that the distribution type of the predicted response value remains unchanged, and the EI function is redefined according to the modified predicted response at the sample point. The selection area of EH function is mainly placed near the LSS and where the variance of the predicted response is large, which can consider both local and global prediction accuracy (Sec. 3.3). Then, a secondary point selection strategy is introduced into the active learning process to increase the model updating efficiency. Based on the initial best point obtained by the improved EGO method, the opposite point across the LSS is found. And between these two points, the final best point with larger expected improvement is selected to update the Kriging metamodel (Sec. 3.4). At last, five classical examples show that the learning function EH and active learning methods proposed in this paper are effective and practical in structural reliability analysis.

2. Kriging metamodel

The Kriging metamodel has been widely used in mechanical, aerospace and other engineering fields in recent years. Generally speaking, Kriging metamodel contains two elements: The polynomial term and the stochastic term [20, 30]. The stochastic process can be the Gauss process, exponential process et al., and the Gauss process is used in this paper. Assume that there is an initial data set $\boldsymbol{x} = [\boldsymbol{x}_1, \boldsymbol{x}_2, ..., \boldsymbol{x}_k]^T$, with $\boldsymbol{x}_i \in R^n (i = 1, 2, ..., k)$ the ith point, and $G = [G(\boldsymbol{x}_1), G(\boldsymbol{x}_2), ..., G(\boldsymbol{x}_k)]^T$ denotes the real responses corresponding to $\boldsymbol{x}$. Then the Kriging metamodel is denoted by

$$\hat{G}(\boldsymbol{x}) = F(\boldsymbol{\beta}, \boldsymbol{x}) + z(\boldsymbol{x}) = f^T(\boldsymbol{x})\boldsymbol{\beta} + z(\boldsymbol{x}) \tag{1}$$

where $\boldsymbol{\beta}^T = [\beta_1, \beta_2, ..., \beta_p]$ is a regression coefficient vector. $f(x) = [f_1(x), f_2(x), ..., f_p(x)]^T$ is a basic polynomial function. The studies have shown that fitting precision of the Kriging doesn't depend on the specific form of $F(\boldsymbol{\beta}, \boldsymbol{x})$. Therefore, $F(\boldsymbol{\beta}, \boldsymbol{x})$ is taken as a constant. $z(\boldsymbol{x})$ is a Gaussian process with zero mean and other characteristics as follows

$$Cov[z(\boldsymbol{x}_i), z(\boldsymbol{x}_j)] = \sigma^2 R(\boldsymbol{\theta}, \boldsymbol{x}_i, \boldsymbol{x}_j) \tag{2}$$

where σ^2 represents the variance of $z(\boldsymbol{x})$. $R(\boldsymbol{\theta}, \boldsymbol{x}_i, \boldsymbol{x}_j)$ defines the special correlation function between $\boldsymbol{x}_i$ and $\boldsymbol{x}_j$, with a correlation parameter vector $\boldsymbol{\theta}$. In this research, the Gaussian correlative function is applied, which can be given by

$$R(\boldsymbol{\theta}, \boldsymbol{x}_i, \boldsymbol{x}_j) = \exp[\sum_{e=1}^{n} [-\theta_e (\boldsymbol{x}_i^e - \boldsymbol{x}_j^e)^2]] \quad \theta_e \geq 0 \tag{3}$$

where n is the dimension of the point. $\boldsymbol{x}_i^e$ and $\boldsymbol{x}_j^e$ are eth components of $\boldsymbol{x}_i$ and $\boldsymbol{x}_j$. θ_e is eth components of $\boldsymbol{\theta}$, which directly affects the prediction results of the metamodel, and it can be obtained by MATLAB toolbox DACE.

Based on k initial experimental sample points set $\boldsymbol{x}$ and corresponding real responses $\boldsymbol{G}$, the regression coefficient $\boldsymbol{\beta}$ and σ^2 are estimated by

$$\hat{\boldsymbol{\beta}} = (\boldsymbol{F}^T \mathbf{R}^{-1} \boldsymbol{F})^{-1} \boldsymbol{F}^T \mathbf{R}^{-1} \boldsymbol{G} \tag{4}$$

$$\hat{\sigma}^2 = \frac{1}{k} (\boldsymbol{G} - \boldsymbol{F}\hat{\boldsymbol{\beta}})^T \mathbf{R}^{-1} (\boldsymbol{G} - \boldsymbol{F}\hat{\boldsymbol{\beta}}) \tag{5}$$

where $\mathbf{R}$ represents the correlation matrix with $\mathbf{R} = [R_{ij}]_{k \times k}$, $R_{ij} = R(\boldsymbol{\theta}, \boldsymbol{x}_i, \boldsymbol{x}_j)$.

At any other point $\boldsymbol{x}$, the unbiased predictor response $\mu_{\hat{G}}(\boldsymbol{x})$

and the predicted variance $\sigma_{\hat{G}}^2(\boldsymbol{x})$ will be denoted by

$$\mu_{\hat{G}}(\boldsymbol{x}) = \hat{G}(\boldsymbol{x}) = \boldsymbol{f}(\boldsymbol{x})^T \hat{\boldsymbol{\beta}} + \boldsymbol{r}(\boldsymbol{x})^T \mathbf{R}^{-1}(\boldsymbol{G} - \boldsymbol{F}\hat{\boldsymbol{\beta}}) \tag{6}$$

$$\hat{\sigma}_{\hat{G}}^2(\boldsymbol{x}) = \hat{\sigma}^2[1 + \boldsymbol{u}(\boldsymbol{x})^T(\boldsymbol{F}^T\mathbf{R}^{-1}\boldsymbol{F})^{-1}\boldsymbol{u}(\boldsymbol{x}) - \boldsymbol{r}(\boldsymbol{x})^T \mathrm{R}^{-1}\boldsymbol{r}(\boldsymbol{x})] \tag{7}$$

where $\boldsymbol{u}(\boldsymbol{x}) = \boldsymbol{F}^{\mathrm{T}}\mathbf{R}^{-1}\boldsymbol{r}\text{-}\boldsymbol{f}$; $\boldsymbol{r}(\boldsymbol{x}) = [R(\boldsymbol{\theta}, \boldsymbol{x}_1, \boldsymbol{x}), R(\boldsymbol{\theta}, \boldsymbol{x}_2, \boldsymbol{x}),..., R(\boldsymbol{\theta}, \boldsymbol{x}_k, \boldsymbol{x})]$. The predicted variance $\hat{\sigma}_{\hat{G}}^2(\boldsymbol{x})$ represents the prediction uncertainty of the metamodel at the sampling point $\boldsymbol{x}$, which is an important basis for the active learning method.

3. Proposed method based on an improved learning function and a new learning method

3.1 The EGO algorithm

The EGO algorithm is a surrogate model optimization for complex problems first proposed by Jones et al. Based on Kriging metamodel, the EI learning function is used to measure the model fitting of the Kriging at an unknown point. The point corresponding to the largest EI function value is picked to update the Kriging metamodel itself, which helps increase the precision of the Kriging model sequentially [23].

For any point $\boldsymbol{x}$ in space, the predicted response $\hat{G}(\boldsymbol{x})$ follows the normal distribution

$$\hat{G}(\boldsymbol{x}) \sim N(\mu_{\hat{G}}(\boldsymbol{x}), \hat{\sigma}_{\hat{G}}(\boldsymbol{x})) \tag{8}$$

Then, the MCS was used to select m points and the corresponding predicted responses were obtained as $\hat{G}_1, \hat{G}_2, ..., \hat{G}_m$. Based on the minimum value $G_{min} = \min(\hat{G}_1, \hat{G}_2, ..., \hat{G}_m)$ of the current surrogate model, the improvement at $\boldsymbol{x}$ is

$$I(\boldsymbol{x}) = \max(G_{min} - \hat{G}(\boldsymbol{x}), 0) \tag{9}$$

where $\hat{G}(x)$ is an uncertain variable, containing the uncertainty of the model fitting at point $\boldsymbol{x}$. Therefore, $I(\boldsymbol{x})$ is also a random variable that the expected improvement (EI) at $\boldsymbol{x}$ is defined as

$$\begin{aligned} E(I(\boldsymbol{x})) &= E(\max(G_{min} - \hat{G}(\boldsymbol{x}), 0)) \\ &= (G_{min} - \hat{G}(\boldsymbol{x}))\Phi(\frac{G_{min} - \hat{G}(\boldsymbol{x})}{\hat{\sigma}_{\hat{G}}(\boldsymbol{x})}) \\ &\quad + \hat{\sigma}_{\hat{G}}(\boldsymbol{x})\phi(\frac{G_{min} - \hat{G}(\boldsymbol{x})}{\hat{\sigma}_{\hat{G}}(\boldsymbol{x})}) \end{aligned} \tag{10}$$

The point $\boldsymbol{x}_{best}$ corresponding to the maximum expected improvement value is recognized as the best point under the current Kriging model. It is expressed as

$$\boldsymbol{x}_{best} = \arg(\max_{\boldsymbol{x}}(E(I(\boldsymbol{x})))) \tag{11}$$

The real response $G(\boldsymbol{x}_{best})$ at point $\boldsymbol{x}_{best}$ is calculated and added to the initial data set to update the Kriging metamodel. Then, larger point set are sampled again under the updated model and carry out a new round of point selection until the iteration stopping condition $(\max(E(I(\boldsymbol{x}))) < 0.001)$ is satisfied.

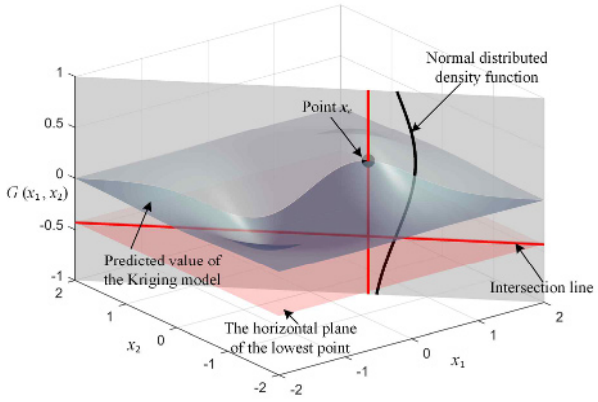

Fig. 1. Graphical analysis of expected improvement in the EGO algorithm.

3.2 The inapplicability of EGO algorithm in structural reliability analysis

Sec. 3.1 shows that the selection strategy of the EGO algorithm is based on the EI function which represents the expected improvement of the metamodel. As shown in Fig. 1, it is a two-dimensional function example, where the response $\hat{G}(\boldsymbol{x}_e)$ at the point $\boldsymbol{x}_e(\boldsymbol{x}_{e1} = 0.5, \boldsymbol{x}_{e1} = -0.5)$ is a Normal random variable $(\hat{G}(\boldsymbol{x}_e) \sim N[\mu_{\hat{G}}(\boldsymbol{x}_e), \hat{\sigma}_{\hat{G}}^2(\boldsymbol{x}_e)])$. The red horizontal plane is the one where the lowest predicted value G_{min} of the Kriging model lies. The black vertical line in the figure represents the probability density distribution function of the response $\hat{G}(\boldsymbol{x}_e)$, and the red horizontal line is the intersection of the lowest horizontal plane and the gray vertical plane. Therefore, the probability of $\hat{G}(\boldsymbol{x}_e) < G_{min}$ is

$$P(G(\boldsymbol{x}_e) < G_{min}) = \phi(\frac{G_{min} - \hat{G}(\boldsymbol{x}_e)}{\hat{\sigma}_{\hat{G}}(\boldsymbol{x}_e)}) \tag{12}$$

The length of the segment under the plane $G(\boldsymbol{x}_e) = G_{min}$ is what we called improvement at point $\boldsymbol{x}_e$. What's more, different improvement corresponds to different probability density function values. In order to measure the expectation of the improvement, the expected improvement (EI) is calculated according to the normal distributed variable $\hat{G}(\boldsymbol{x}_e)$, which can be defined as

$$\begin{aligned} E\left(I\left(\boldsymbol{x}_e\right)\right) &= (G_{min} - \hat{G}(\boldsymbol{x}_e))\Phi(\frac{G_{min} - \hat{G}(\boldsymbol{x}_e)}{\hat{\sigma}_{\hat{G}}(x)}) \\ &\quad + \hat{\sigma}_{\hat{G}}(\boldsymbol{x}_e)\phi(\frac{G_{min} - \hat{G}(\boldsymbol{x}_e)}{\hat{\sigma}_{\hat{G}}(\boldsymbol{x}_e)}) \end{aligned} \tag{13}$$

As shown in Eq. (13) and Fig. 1 that two main factors are af-

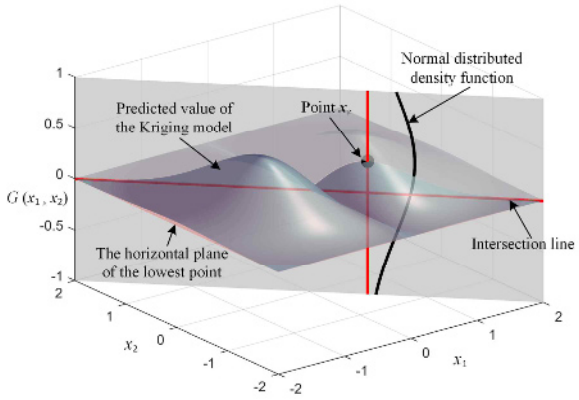

Fig. 2. Graphical analysis of expected improvement in the IEGO algorithm.

fecting the expected improvement $E(I(\boldsymbol{x}_e))$: 1) The predicted response value $\hat{G}(\boldsymbol{x}_e)$, i.e. the mean of the normal distribution. Assuming that the variance $\hat{\sigma}^2_{\hat{G}}(\boldsymbol{x}_e)$ remains unchanged, and the smaller the $\hat{G}(\boldsymbol{x}_e)$ is, the closer the distance between the plane $G(\boldsymbol{x}) = G_{min}$ and mean $\hat{G}(\boldsymbol{x}_e)$. According to the characteristics of the normal function, the expected improvement value also increases. 2) The standard deviation $\hat{\sigma}^2_{\hat{G}}(\boldsymbol{x}_e)$, which indicates the uncertainty of predicted response value. Assuming that the mean $\hat{G}(\boldsymbol{x}_e)$ remains unchanged, the larger the $\hat{\sigma}_{\hat{G}}(\boldsymbol{x}_e)$ is, the more dispersed the normal distribution function is, which results in the increases of both the probability density function value at the plane $G(\boldsymbol{x}) = G_{min}$ and expected improvement.

In summary, the point selection strategy of the classical EGO algorithm is to select points with small response value and larger standard deviation as the best next updating of Kriging metamodel. However, it is not in line with the concept of structural reliability analysis. In the process of reliability index evaluation, we are mainly concerned with the fitting accuracy of the region near the LSS, not the minimum of the response surface. Hence, directly using the EI function as the active learning in reliability analysis will result in an insufficient selection of points and a larger error in reliability analysis.

3.3 The improved EGO algorithm (IEGO)

In this paper, an improved EGO (IEGO) algorithm is proposed. By changing the definition of the expected improvement $E(I(\boldsymbol{x}))$, the point selection strategy can focus on not only the points nearby the LSS, but also the points with large variance. As shown in Fig. 2, the two-dimensional function in Sec. 2.1 is still provided for describing. Based on the predicted value of surrogate metamodel, the part of $\hat{G}(\boldsymbol{x}) < 0$ will be flipped according to the plane $\hat{G}(\boldsymbol{x}) = 0$. In other words, the new distribution mean $\hat{Y}(\boldsymbol{x})$ of the random variable $\hat{G}(\boldsymbol{x})$ is

$$\hat{Y}(\boldsymbol{x}) = \begin{cases} \hat{G}(\boldsymbol{x}) & \hat{G}(\boldsymbol{x}) \geq 0 \\ -\hat{G}(\boldsymbol{x}) & \hat{G}(\boldsymbol{x}) < 0 \end{cases} \tag{14}$$

Then, it is assumed that the variance of the predicted response at point $\boldsymbol{x}_e$ remains unchanged. Therefore, it can be considered that the modified predicted value $\hat{G}(\boldsymbol{x}_e)$ at point $\boldsymbol{x}_e$ follows the normal distribution $N[\hat{Y}(\boldsymbol{x}_e), \ \hat{\sigma}^2_{\hat{G}}(\boldsymbol{x}_e)\ ]$. And, the minimum of the predicted response value is redefined as

$$Y_{min} = \min\left(|\hat{G}_1|, |\hat{G}_2|, \ldots, |\hat{G}_m|\right) \tag{15}$$

Since the candidate points generally exist in both safety and failure domains, the minimum value can be further defined as

$$Y_{min} = 0 \tag{16}$$

And, the new improvement function is denoted as

$$H(\boldsymbol{x}_e) = \max(Y_{\min} - \hat{Y}(\boldsymbol{x}_e), 0) \tag{17}$$

Therefore, the improved expected improvement EH can be derived as

$$\begin{aligned} &EH(\boldsymbol{x}_e) \\ &= E[\max(Y_{min} - \hat{Y}(\boldsymbol{x}_e), 0)] \\ &= \int_0^{+\infty} H(\boldsymbol{x}) \{ \frac{1}{\sqrt{2\pi}\hat{\sigma}_{\hat{G}}(\boldsymbol{x})} * \exp[\frac{-(Y_{min} - H(\boldsymbol{x}) - \hat{Y}(\boldsymbol{x}))^2}{2\hat{\sigma}_{\hat{G}}{}^2(\boldsymbol{x})}] \} dH(\boldsymbol{x}) \Big|_{x=x_e} \\ &= (-\hat{Y}(\boldsymbol{x}_e))\Phi(\frac{-\hat{Y}(\boldsymbol{x}_e)}{\hat{\sigma}_{\hat{G}}(\boldsymbol{x}_e)}) + \hat{\sigma}_{\hat{G}}(\boldsymbol{x}_e)\phi(\frac{-\hat{Y}(\boldsymbol{x}_e)}{\hat{\sigma}_{\hat{G}}(\boldsymbol{x}_e)}) \end{aligned} \tag{18}$$

In Eq. (18), the first item of the equation on the right side is the improvement at point $\boldsymbol{x}_e$ multiplied by the normal cumulative distribution function at Y_{min}. Therefore, the search focus is placed near the LSS, which greatly strengthens the local search capability. And the second item of the equation on the right side is the prediction uncertainty ($\sigma_{\hat{G}}(\boldsymbol{x}_e)$) multiplied by the normal probability density function at Y_{min}. In other words, the region with low prediction accuracy will become a key search area, which strengthens the global search ability of IEGO algorithm.

3.4 Secondary point selection strategy based on IEGO algorithm

A simple active learning strategy only seeks the point with the optimal assessment index (like the expected improvement) as the optimal point among the candidate data set, which may lead to inaccurate and inefficiency selection. And, if there is one point with two properties: Close to the optimal point (obtained by active learning strategy) and has a larger expected improvement value, which may better update the Kriging model. According to this idea, a secondary point selection strategy based on the IEGO algorithm is raised in this paper.

The optimal point obtained from the IEGO algorithm is defined as the initial best point $\boldsymbol{x}_{ib}$. And, it is obvious that there are

two cases of $\boldsymbol{x}_{ib}$(as shown in Fig. 3):

(1) the point $\boldsymbol{x}_{ib}$ is in the safer domain. Taking the initial best point as the starting point, iterating along the negative gradient direction (i.e. the blue direction indictor in Fig. 3) with the unit step length. Therefore, the iterative direction and step length of the kth iteration are

$$\begin{cases} \boldsymbol{d}^{(k)} = -\dfrac{\nabla g(\boldsymbol{u}^{(k)})}{\| \nabla g(\boldsymbol{u}^{(k)}) \|} \\ \lambda^{(k)} = 1 \end{cases} \qquad k = 1,2,3,... \tag{19}$$

where $\boldsymbol{u}^{(k)}$ represents the origin of the kth iteration.

(2) the point $\boldsymbol{x}_{ib}$ is in the failure domain. In this case, $\boldsymbol{x}_{ib}$ is still used as the starting point, while the gradient direction (i.e. the red direction indictor in Fig. 3) and unit step length are adopted for iteration. Therefore, the iterative direction and step length at the kth iteration are

$$\begin{cases} \boldsymbol{d}^{(k)} = \dfrac{\nabla g(\boldsymbol{u}^{(k)})}{\| \nabla g(\boldsymbol{u}^{(k)}) \|} \\ \lambda^{(k)} = 1 \end{cases} \qquad k = 1,2,3,... \tag{20}$$

And, the iteration continues until the point $\boldsymbol{x}_{opp}$ opposite to the sign of the predicted value of point $\boldsymbol{x}_{ib}$ is obtained for the first time. After that, searching for the final best point $\boldsymbol{x}_{fb}$ becomes an optimization problem, which can be expressed as

$$\begin{aligned} &\max_{\boldsymbol{x}_i}(EH(\boldsymbol{x}_i)) \qquad i = 1,2,\cdots,p+1 \\ &s.t. \quad \boldsymbol{x}_i = \boldsymbol{x}_{ib} \cdot m + \boldsymbol{x}_{opp} \cdot (1-m), \quad 0 \le m \le 1 \end{aligned} \tag{21}$$

where $\boldsymbol{x}_i$ is one point uniformly distributed on the line between point $\boldsymbol{x}_{ib}$ and point $\boldsymbol{x}_{opp}$, p represents the size of the points set. Obviously, the smaller value of p will lead to a more insufficient sample size of a uniformly distributed point set. But with a larger value of p, it will greatly increase the amount of calculation in the process of searching for the final best point. Thus, 1000 is applied to p.

3.5 Main computational steps

Combined with the Kriging and the model updating method raised in Secs. 3.3 and 3.4, the major steps of the proposed method are described as follows:

(1) Through MCS simulation, N_{MC} random samples $\boldsymbol{S}_{MC} = [\boldsymbol{x}_1, \boldsymbol{x}_2, ..., \boldsymbol{x}_{NMC}]^T$ are generated according to the joint distribution of the basic variables. And the $\boldsymbol{S}_{MC}$ will be used as the candidate samples in the active learning process, called candidate data set.

(2) LHS method is adopted to generate initial point set $\boldsymbol{S}_{\text{initial}} = [\boldsymbol{x}_1, \boldsymbol{x}_2, ..., \boldsymbol{x}_N]^T$ for the preliminary fitting of Kriging metamodel in the basic random variables space $(\mu_i - 3\sigma_i, \mu_i + 3\sigma_i)$, $i = 1, 2, ..., n$. The size N of the point set $\boldsymbol{S}_{initial}$ should be selected appropriately, and the $\boldsymbol{S}_{initial}$ will be updated continuously in the process of the subsequent learning process.

Table 1. Evaluation results of the example 1.

Algorithm	N_{call}	$P_f(10^{-3})$	$\varepsilon(\%)$
MCS	10^7	3.4453	-
Proposed method	39	3.5230	2.26
IEGO	39	3.5573	3.25
U	57	3.4700	0.72
EFF	29	3.2177	6.61

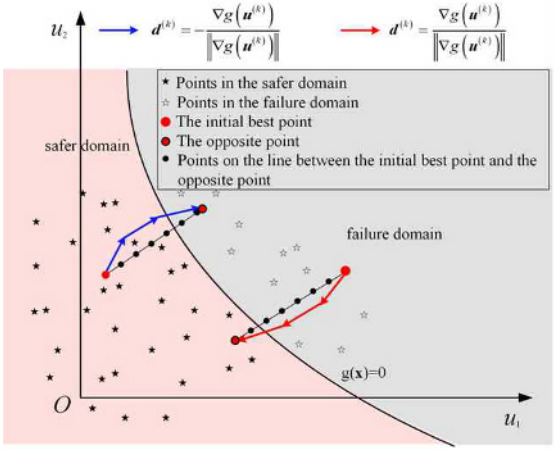

Fig. 3. Diagram of the secondary point selection strategy.

(3) Calling the performance function to evaluate the real response set $\boldsymbol{G}_{initial}$ corresponding to the $\boldsymbol{S}_{initial}$, and the Kriging metamodel is established. Through the surrogate model, the predicted values $\hat{G}(\boldsymbol{x}_i)$, $\boldsymbol{x}_i \in \boldsymbol{S}_{MC}$ and standard deviation $\sigma_{\hat{G}}(\boldsymbol{x}_i)$, $\boldsymbol{x}_i \in \boldsymbol{S}_{MC}$ are estimated.

(4) According to Eqs. (14) and (16), the modified predicted value $\hat{Y}(\boldsymbol{x}_i)$, $\boldsymbol{x}_i \in \boldsymbol{S}_{MC}$ and the current minimum values $\boldsymbol{Y}_{min}$ are calculated, which is used to estimate the improved expected improvement $EH(\boldsymbol{x}_i)$, $\boldsymbol{x}_i \in \boldsymbol{S}_{MC}$. And, get the initial best point $\boldsymbol{x}_{ib}$ corresponding to the $\max(EH(\boldsymbol{x}_i))$, $\boldsymbol{x}_i \in \boldsymbol{S}_{MC}$.

(5) Starting from the point $\boldsymbol{x}_{ib}$, search for the opposite point corresponding to $\boldsymbol{x}_{ib}$ by the method mentioned in Sec. 3.4. And carry out the secondary point selection between these two points to get the final best point $\boldsymbol{x}_{fb}$.

(6) If $\max(EH(\boldsymbol{x}_i)) < 0.001$, $\boldsymbol{x}_i \in \boldsymbol{S}_{MC}$, the active learning process ends and the failure probability is estimated in step 7). Otherwise, evaluate the real response $\boldsymbol{G}(\boldsymbol{x}_{fb})$ of the final best point $\boldsymbol{x}_{fb}$, which will be added into the $\boldsymbol{S}_{initial}$ and $\boldsymbol{G}_{initial}$, and back to step 3).

(7) Based on the MCS method, the final Kriging metamodel is adopted to evaluate the probability of failure P_f and variation coefficient δ_{Pf}

$$\delta_{P_f} = \sqrt{\frac{1-P_f}{(N_{MC}-1)P_f}} \tag{22}$$

and the iteration converges when $\delta_{Pf} < 0.03$ is satisfied.

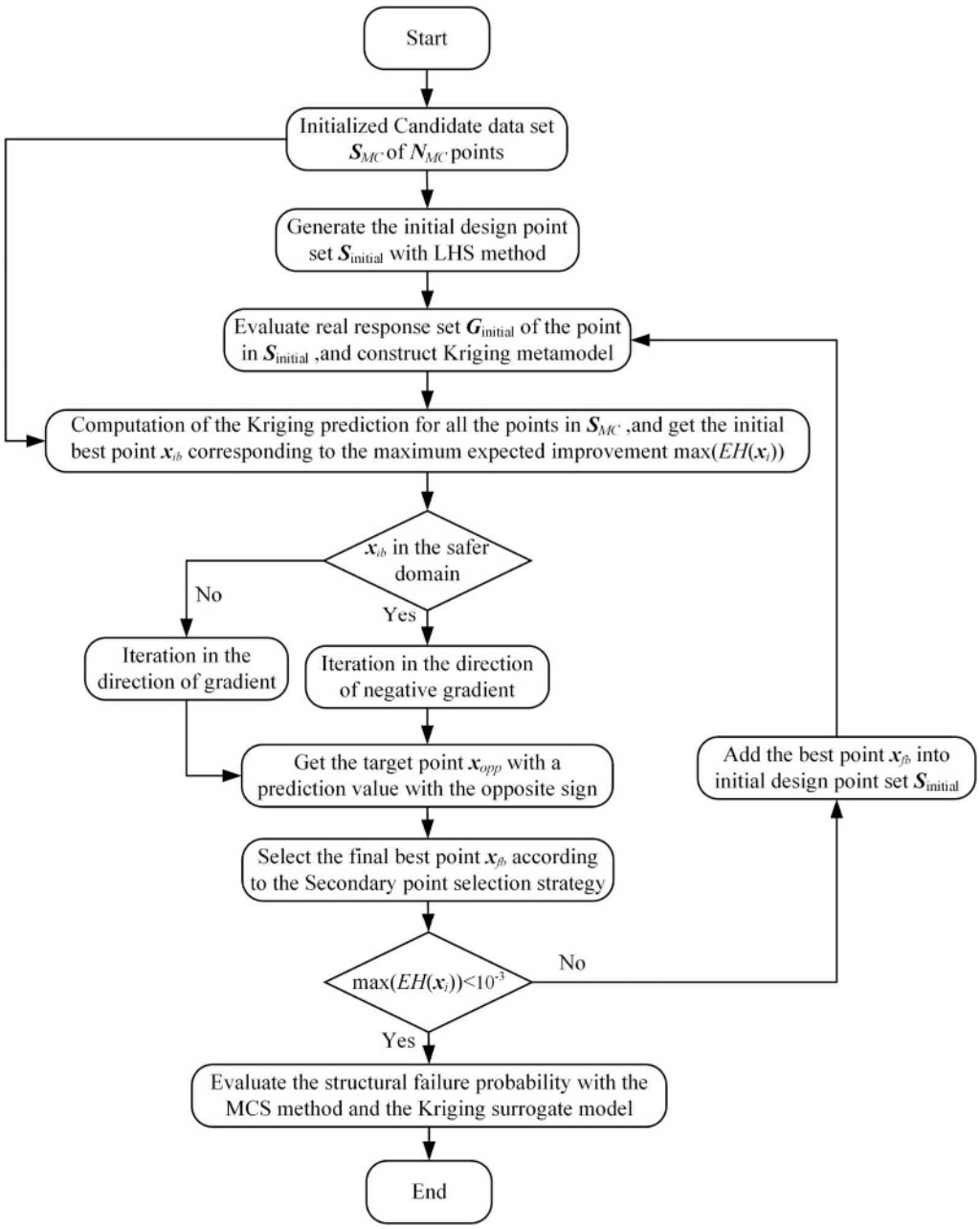

Fig. 4. The flow diagram of the proposed method.

4. Validation examples

For purpose of verifying the precision and validity of the proposed method, five practical examples are presented, including two mathematical examples and three engineering examples. These four reliability analysis methods all evaluate the failure probability by the MCS method with 1×10^7 sample points. In each example, the results of MCS method P_f^{MC} is regarded as the standard solution, and the proposed method is compared with IEGO, EFF and U algorithm from the following two aspects: 1) With the same size of initial design point set, the amount N_{call} of calling the performance function is taken to measure the calculation efficiency of each method. 2) The relative error between the failure probability P_f acquired by each method and P_f^{MC} are used to represent the calculation accuracy, which is calculated as

$$\varepsilon = \frac{|P_f - P_f^{MC}|}{P_f^{MC}} \tag{23}$$

4.1 Example 1

Here is a nonlinear system with two performance function [31, 32], it is defined as

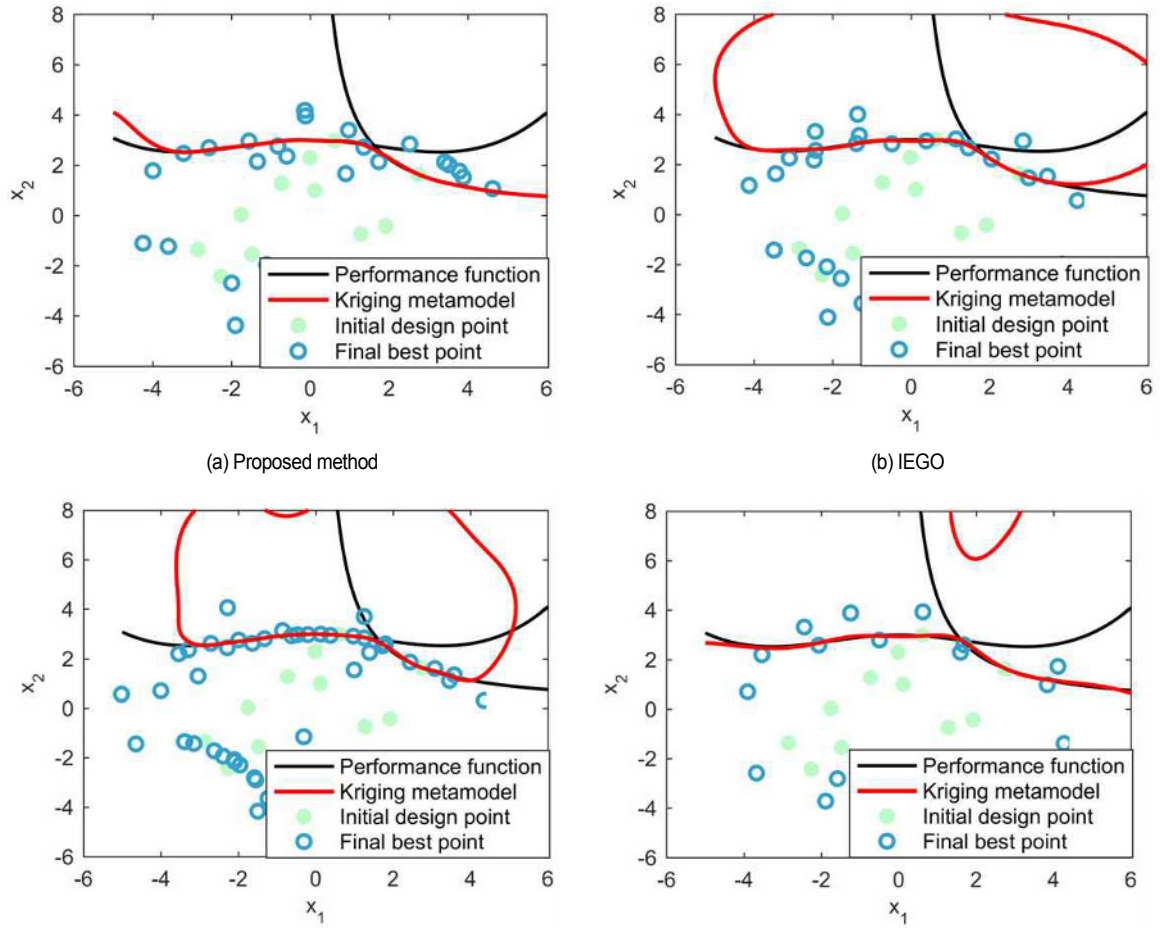

(a) Proposed method (b) IEGO

(c) U (d) EFF

Fig. 5. Comparison among the proposed method, IEGO, U and EFF algorithm corresponds to (a)-(d) for example 1.

$$g(x_1,x_2)=\min\begin{cases}3-1-x_2+\exp(-\dfrac{x_1^2}{10})+(\dfrac{x_1}{5})^5\\ \dfrac{3^2}{2}-x_1x_2\end{cases} \tag{24}$$

where x_1 and x_2 are both subject to $N(0,1)$ and independent of each other. The analysis results are summarized in Table 1 and the learning process of different active learning method are shown in Fig. 5.

As shown in Table 1, the EFF algorithm calls the minimum number of performance functions but with the maximum relative error. The computational effort of the U algorithm is a little larger, result in low calculation efficiency. The calling number of the proposed method and IEGO are the same since it is a relatively simple mathematical example, but the proposed method has a higher calculation accuracy than IEGO algorithm.

For purpose of demonstrating the fitting accuracy more intuitively, the learning process of these four methods are compared in Fig. 5. The initial design points (green dots), the final best points (blue circle) and the LSS of both real performance function (black solid line) and Kriging model (red solid line) are all plotted in Fig. 5. From Figs. 5(a)-(d), it can be seen that the fitting of the EFF algorithm near the LSS is unsatisfactory due to the immature convergence. The U algorithms has a high fitting accuracy, but with the point accumulation near the LSS. The proposed method is relatively reasonable in selecting points near the LSS and with a similar fitting accuracy.

4.2 Example 2

This example considers a series system with four performance function [12, 19, 33, 34], which can be given as

$$g(x_1,x_2)=\min\begin{Bmatrix}3+\dfrac{(x_1-x_2)^2}{10}-\dfrac{(x_1+x_2)}{\sqrt{2}}\\ 3+\dfrac{(x_1-x_2)^2}{10}+\dfrac{(x_1+x_2)}{\sqrt{2}}\\ (x_1-x_2)+\dfrac{7}{\sqrt{2}}\\ (x_2-x_1)+\dfrac{7}{\sqrt{2}}\end{Bmatrix} \tag{25}$$

where x_1 and x_2 are both subject to $N(0,1)$ and independent of

each other. The analysis results are summarized in Table 2 and the learning process of different active learning algorithm are shown in Fig. 6.

As shown in Table 2, the raised method can obtain a highest accuracy results with a lower number of performance function calls among these four algorithms. The relative error of the EFF algorithm is more than 10 % which is unacceptable in practical engineering no matter how efficient the algorithm is.

Like example1, the active learning process of different methods is also plotted in Fig. 6. Both Figs. 6(a) and (b) validate the effectiveness of IEGO algorithm in reliability analysis, and the comparison of these two also shows that the secondary point selection strategy can futher improve the computational efficiency. Besides, the point selection of U algorithm is too dense near the LSS, which will result in a large calculation consumption in practical engineering applications. As demonstrated in the Fig. 6(d), the EFF algorithm has relatively poor-fitting because of too few points selection.

Table 2. Evaluation results of the example 2.

Algorithm	N_{call}	$P_f(10^{-3})$	$\varepsilon(\%)$
MCS	10^7	2.2091	-
Proposed method	59	2.2167	0.34
IEGO	69	2.2081	0.45
U	77	2.2392	1.36
EFF	38	2.4361	10.28

4.3 Example 3

The ten-bar truss structure is applied in this example seen in Fig. 7 [35]. There are three kinds of the bars: horizontal, diagonal and vertical bar, which has different cross-sectional areas among each other. Hence, the design variables S_1, S_2 and S_3 corresponding to the cross-sectional of horizontal, diagonal and vertical ones are regarded as normally distributed random variables. And, $S_1 \sim N(13,1.3)$ in^2, $S_2 \sim N(2,0.2)$ in^2, $S_3 \sim N(9,0.9)$ in^2. The other deterministic parameters are shown in Table 3.

With the finite element analysis technology, the analytical expression for the displacement at node (2) is derived as follows:

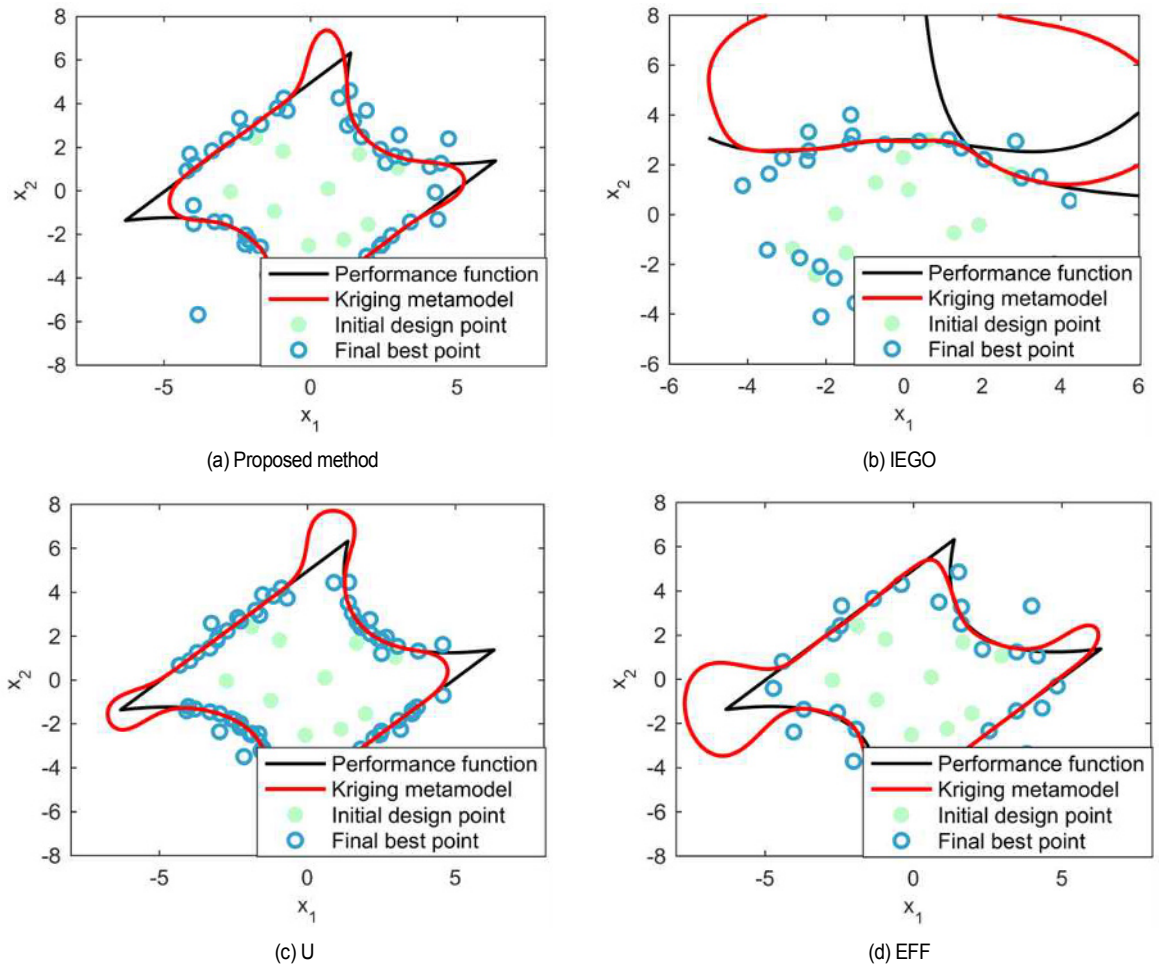

(a) Proposed method (b) IEGO

(c) U (d) EFF

Fig. 6. Comparison among the proposed method, IEGO, U, and EFF algorithm corresponds to (a)-(d) for example 2.

Table 3. The deterministic parameters of the ten-bar truss.

Parameters	Value
Force P(lb)	100000
Length L(in)	360
Young's modulus E(psi)	10^7
Material density ρ(lb/in^3)	0.1

Table 4. Evaluation analysis results of the example 3.

Algorithm	N_{call}	P_f	ε(%)
MCS	10^7	0.1729	-
Proposed method	18	0.1739	0.57
IEGO	21	0.1730	0.05
U	33	0.1730	0.05
EFF	22	0.1704	1.44

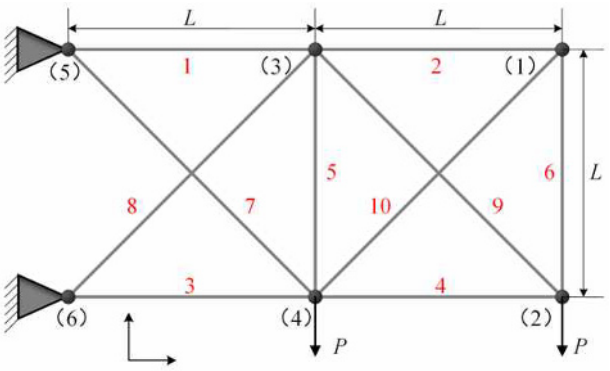

Fig. 7. Ten-bar truss structure.

$$g_{disp}=\frac{PL}{S_1S_3E}\{\frac{4\sqrt{2}S_1^3(24S_2^2+S_3^2)+S_3^3(7S_1^2+26S_2^2)}{D_T}+\frac{4S_1S_2S_3[(20S_1^2+76S_1S_2+10S_3^2)+\sqrt{2}S_3(25S_1+29S_2)]}{D_T}\}-d_{allow} \tag{26}$$

where $d_{allow}=4$ in, and the D_T is expressed by

$$D_T=4S_2^2(8S_1^2+S_3^2)+4\sqrt{2}S_1S_2S_3(3S_1+4S_2)+S_1S_3^2(S_1+6S_2) \tag{27}$$

All the reliability analysis results are summarized in Table 4.

Obviously, the proposed method based on the IEGO algorithm makes the least calls to the performance function and has an acceptable calculation error. Compared with the U algorithm, the IEGO algorithm calls the performance function more than ten times less and gets a result with the same precision. And as in the previous example, the relative error of the EFF algorithm is largest among all these four algorithms.

4.4 Example 4

The front axle beam is a front support bracket of the automobile (shown in Fig. 8) [36, 37]. And, the I-beam structure of front axle is the most popular design because of its lightweight and high bend strength. In general, a fracture section may occur in the middle part of the I-beam which is seen in Fig. 8.

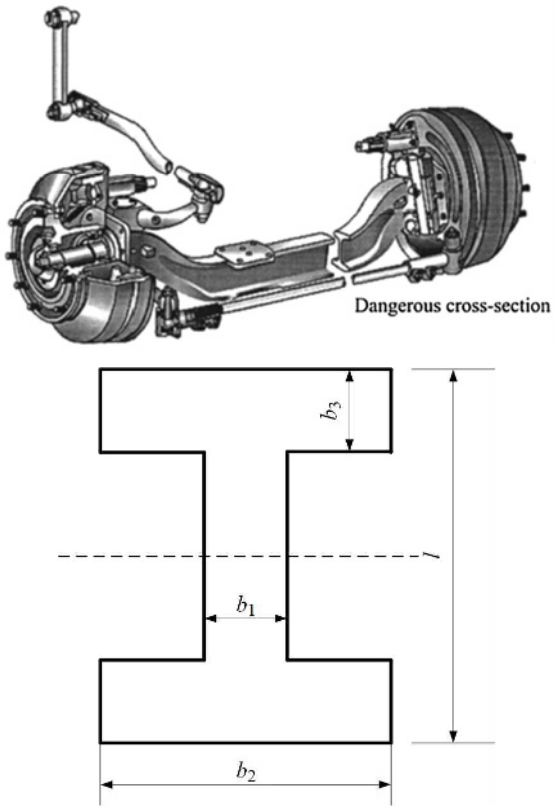

Fig. 8. The automobile front axle.

The section factor W_s and W_p polar section factor of the I-beam structure are defined as

$$W_s=\frac{b_1(l-2b_3)^3}{6l}+\frac{b_2}{6l}[l^3-(l-2b_3)^3] \tag{28}$$

$$W_p=0.8b_2b_3^{\ 2}+0.4b_1^{\ 3}\frac{(l-2b_3)}{b_3} \tag{29}$$

According to the stress, the maximum normal stress and shear stress can be expressed by

$$\sigma_I=\frac{M_I}{W_s} \tag{30}$$

$$\tau_I=\frac{T_I}{W_p} \tag{31}$$

where M_I and T_I represent the bending moment and torque, respectively.

And the performance function is derived as follows to assess the static strength of the front axle.

$$g=\sigma_s-\sqrt{\sigma_I^2+3\tau_I^2} \tag{32}$$

Table 5. Distributions of random variables.

Random variables	Mean	Coefficient of variation
b_1	12	0.005
b_2	65	0.005
b_3	14	0.005
l	85	0.005
M_I	3.5×10^6	0.05
T_I	3.1×10^6	0.05

Table 6. Evaluation analysis results of the example 4.

Algorithm	N_{call}	$P_f(10^{-2})$	$\varepsilon(\%)$
MCS	10^7	1.9434	-
Proposed method	31	1.9511	0.40
IEGO	38	1.9487	0.27
U	37	1.9522	0.45
EFF	25	1.9591	0.81

where σ_s represents the limiting yield stress and takes 460 MPa under comprehensive consideration. The corresponding distribution information of the independent normal variables (unit: mm) b_1, b_2, b_3, l and the loads variables (unit: N·mm) M_I and T_I are listed in Table 5.

Apply these four methods to the front axle beam example, and the analysis results is summarized in Table 6. It can be observed that the calculation efficiency of the proposed method is better than IEGO and U algorithm. And, the calculation error of the proposed method is nearly half as small as the EFF algorithm, in the case that the performance function is called only 6 times more than the EFF algorithm.

4.5 Example 5

In this case, a non-linear oscillator is applied for analysis as shown in Fig. 9 [25, 38]. And, the performance function is denoted by

$$g(M,K_1,K_2,R,T_1,F_1)=3R-\left|\frac{2F_1}{M\omega^2}\sin\left(\frac{\omega^2T_1}{2}\right)\right| \tag{33}$$

where

$$\omega=\sqrt{(K_1+K_2)/M} \tag{34}$$

The corresponding distribution information of the six independent normal variables K_1, K_2, M, R, T_1, F_1 are listed in Table 7 and the analysis results are summarized in Table 8.

From the results in Table 8, the N_{call} of the IEGO algorithm is 87 times which is 8 times less than the U algorithm. Further, the proposed method only calls the performance function 66 times, about 30 % less than the U algorithm. What's more, in terms of the calculation accuracy, the proposed method is minimum among all these four algorithms. It is fully explained that the proposed method based on the IEGO algorithm can well balance the calculation efficiency and accuracy in the practical reliability engineering.

Table 7. Distributions of random variables.

Random variables	Mean	Coefficient of variation
M	1	0.05
K_1	1	0.1
K_2	0.1	0.1
R	0.5	0.1
T_1	1	0.2
F_1	1	0.2

Table 8. Evaluation analysis results of the example 5.

Algorithm	N_{call}	$P_f(10^{-2})$	$\varepsilon(\%)$
MCS	10^7	3.8692	-
Proposed method	66	3.8787	0.25
IEGO	87	3.8953	0.67
U	95	3.8360	0.86
EFF	32	3.9215	1.35

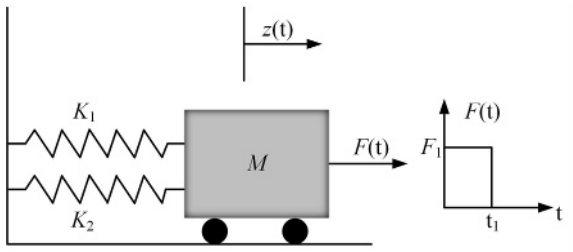

Fig. 9. Non-linear oscillator.

5. Conclusions

In this paper, an improved efficient global optimization (IEGO) and a new secondary point selection strategy are proposed for Kriging metamodel. The IEGO algorithm can give priority to local selection in important regions to ensure the fitting accuracy of Kriging metamodel near the LSS. At the same time, the points with larger predicted variance can also be taken into account to avoid the overfitting of the surrogate model. Then, the secondary point selection strategy is raised to further select the optimal points locally between the initial best point obtained from the IEGO algorithm and the LSS, in which the point closer to the LSS and with greater prediction variance is obtained.

Finally, the feasibility of the raised method is verified by two mathematical examples and three classical engineering problems. And, the final results show that under the same framework of structural reliability analysis: 1) The raised EH function

can meet the requirements of active learning in reliability analysis. And compared with the U algorithm and EFF algorithm, the EH active learning function can better balance the calculation efficiency and accuracy, which is more applicable for practical reliability engineering. 2) The secondary point selection strategy based on the IEGO algorithm mentioned in this paper can further reduce the computational cost without excessively losing calculation accuracy.

Acknowledgments

The financial supports from the National Science and Technology Major Project of China (Grant No. 2017-V-0013-0065 and Grant No.2017-V-0010-0060) are gratefully acknowledged.

References

[1] Y. T. Wu, Computational methods for efficient structural reliability and reliability sensitivity analysis, *AIAA Journal*, 32 (8) (1994) 1717-1723.

[2] S. K. Au, Reliability-based design sensitivity by efficient simulation, *Computers & Structures*, 83 (14) (2005) 1048-1061.

[3] C. Tong, Z. L. Sun and Q. L. Zhao, A hybrid algorithm for reliability analysis combining Kriging and subset simulation importance sampling, *Journal of Mechanical Science and Technology*, 29 (8) (2015) 3183-3193.

[4] B. Echard et al., A combined importance sampling and Kriging reliability method for small failure probabilities with time-demanding numerical models, *Reliability Engineering and System Safety*, 111 (8) (2013) 232-240.

[5] G. I. Schuëller, H. J. Pradlwarter and P. S. Koutsourelakis, A critical appraisal of reliability estimation procedures for high dimensions, *Probabilistic Engineering Mechanics*, 19 (4) (2004) 463-473.

[6] J. Morio et al., A survey of rare event simulation methods for static input-output models, *Simulation Modelling Practice and Theory*, 49 (2014) 287-304.

[7] R. Rackwitz and B. Fiessler, Structural reliability under combined random load sequences, *Computers & Structures*, 9 (5) (1978) 489-494.

[8] F. F. Xiong et al., A double weighted stochastic response surface method for reliability analysis, *Journal of Mechanical Science and Technology*, 26 (8) (2012) 2573-2580.

[9] D. Q. Zhang et al., Time-dependent reliability analysis through response surface method, *Journal of Mechanical Design*, 139 (4) (2017) 041404.

[10] D. L. Allaix and V. I. Carbone. An improvement of the response surface method, *Structural Safety*, 33 (2) (2011) 165-172.

[11] H. Z. Dai et al., Structural reliability assessment by local approximation of limit state functions using adaptive markov chain simulation and support vector regression, *Computer-Aided Civil and Infrastructure Engineering*, 27 (9) (2012) 676-686.

[12] J. M. Bourinet, F. Deheeger and M. Lemaire, Assessing small failure probabilities by combined subset simulation and support vector machines, *Structural Safety*, 33 (6) (2011) 343-353.

[13] H. Z. Dai, H. Zhang and W. Wang, A support vector density-based importance sampling for reliability assessment, *Reliability Engineering & System Safety*, 106 (2012) 86-93.

[14] J. Cheng et al., A new approach for solving inverse reliability problems with implicit response functions, *Engineering Structures*, 29 (1) (2007) 71-79.

[15] V. Papadopoulos et al., Accelerated subset simulation with neural networks for reliability analysis, *Computer Methods in Applied Mechanics and Engineering*, 223-224 (2012) 70-80.

[16] G. B. Kingston et al., Computational intelligence methods for the efficient reliability analysis of complex flood defence structures, *Structural Safety*, 33 (1) (2011) 64-73.

[17] S. Choi, G. Lee and I. Lee, Adaptive single-loop reliability-based design optimization and post optimization using constraint boundary sampling, *Journal of Mechanical Science and Technology*, 32 (7) (2018) 3249-3262.

[18] S. Lee and J. H. Kim, An adaptive importance sampling method with a Kriging metamodel to calculate failure probability, *Journal of Mechanical Science and Technology*, 31 (12) (2017) 5769-5778.

[19] B. Echard, N. Gayton and M. Lemaire, AK-MCS: An active learning reliability method combining Kriging and Monte Carlo simulation, *Structural Safety*, 33 (2) (2011) 145-154.

[20] G. Matheron, The intrinsic random functions and their applications, *Advances in Applied Probability*, 5 (3) (1973) 439-468.

[21] Z. Liu et al., Hybrid structure reliability method combining optimized Kriging model and importance sampling, *Acta Aeronautica et Astronautica Sinica*, 34 (6) (2013) 1347-1355.

[22] J. Wei, J. G. Zhang and T. Qiu, Structural reliability algorithm based on improved dynamic Kriging model, *Journal of Beijing University of Aeronautics and Astronautics*, 45 (2) (2019) 373-380.

[23] D. R. Jones, M. Schonlau and W. J. Welch, Efficient global optimization of expensive black-Box functions, *Journal of Global Optimization*, 13 (4) (1998) 455-492.

[24] B. J. Bichon et al., Efficient global reliability analysis for nonlinear implicit performance functions, *AIAA Journal,* 46 (10) (2008) 2459-2468.

[25] Z. Y. Lv, Z. Z. Lu and P. Wang, A new learning function for Kriging and its application to solve reliability problems in engineering, *Computers & Mathematics with Applications*, 70 (5) (2015) 1182-1197.

[26] M. Balesdent, J. Morio and J. Marzat, Kriging-based adaptive importance sampling algorithms for rare event estimation, *Structural Safety*, 44 (2334) (2013) 1-10.

[27] X. X. Huang, J. Q. Chen and H. P. Zhu, Assessing small failure probabilities by AK-SS: An active learning method combining Kriging and Subset simulation, *Structural Safety*, 59 (2016) 86-95.

[28] I. Depina et al., Reliability analysis with metamodel line sampling, *Structural Safety*, 60 (2016) 1-15.

[29] W. Y. Yun, Z. Z. Lu and X. Jiang, An efficient reliability analysis method combing adaptive Kriging and modified importance

sampling for small failure probability, *Structural and Multidisciplinary Optimization*, 58 (2018) 1383-1393.
[30] J. Sacks, S. B. Schiller and W. J. Welch, Design for computer experiment, *Technometrics*, 31 (1) (1989) 41-47.
[31] H. L. Zhao et al., An efficient reliability method combining adaptive importance sampling and Kriging metamodel, *Applied Mathematical Modelling*, 39 (7) (2015) 1853-1866.
[32] X. K. Yuan et al., A novel adaptive importance sampling algorithm based on Markov chain and low-discrepancy sequence, *Aerospace Science and Technology*, 29 (1) (2013) 253-261.
[33] Z. L. Sun et al., LIF: A new Kriging based learning function and its application to structural reliability analysis, *Reliability Engineering & System Safety*, 157 (2017) 152-165.
[34] F. Cadini, F. Santos and E. Zio, An improved adaptive Kriging-based importance technique for sampling multiple failure regions of low probability, *Reliability Engineering & System Safety*, 131 (8) (2014) 109-117.
[35] B. Keshtegar and Z. Meng, A hybrid relaxed first-order reliability method for efficient structural reliability analysis, *Structural Safety*, 66 (2017) 84-93.
[36] P. Wang, Z. Z. Lu and Z. C. Tang, An application of the Kriging method in global sensitivity analysis with parameter uncertainty, *Applied Mathematical Modelling*, 37 (9) (2013) 6543-6555.
[37] W. Y. Yun et al., A novel step-wise AK-MCS method for efficient estimation of fuzzy failure probability under probability inputs and fuzzy state assumption, *Engineering Structures*, 183 (2019) 340-350.
[38] P. J. Zheng et al., A new active learning method based on the learning function U of the AK-MCS reliability analysis method, *Engineering Structures*, 148 (2017) 185-194.

Hong Linxiong is a Ph.D. candidate in the School of Power and Energy, Northwestern Polytechnical University. His research interests include structural reliability, aero-engine fuel system and others.